

AD-A162 387

UNDERSTANDING THE HIP (HOT ISOSTATIC PRESSING)
CONSOLIDATION OF P/M NICKEL (U) COLUMBIA UNIV NEW YORK
CENTER FOR STRATEGIC MATERIALS J K TIEN 19 JUN 85

1/1

UNCLASSIFIED

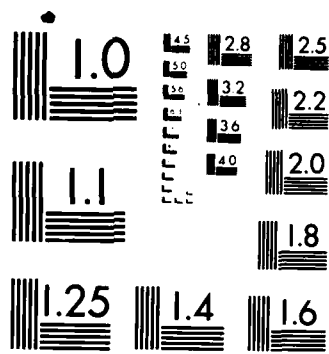
AFOSR-TR-85-0984 AFOSR-82-0352

F/G 11/6

ML



			END
			FM MED
			DTIC



MICROCOPY RESOLUTION TEST CHART
NATIONAL BUREAU OF STANDARDS 1963-A

2

AD-A162 387

UNCLASSIFIED

SECURITY CLASSIFICATION OF THIS PAGE

REPORT DOCUMENTATION PAGE

1a. REPORT SECURITY CLASSIFICATION UNCLASSIFIED		1b. RESTRICTIVE MARKINGS	
2a. SECURITY CLASSIFICATION AUTHORITY		3. DISTRIBUTION/AVAILABILITY OF REPORT <i>Approved for public release; distribution unlimited.</i>	
2b. DECLASSIFICATION/DOWNGRADING SCHEDULE		5. MONITORING ORGANIZATION REPORT NUMBER(S) AFOSR-TR- 82-0352	
4. PERFORMING ORGANIZATION REPORT NUMBER(S)		7a. NAME OF MONITORING ORGANIZATION Same as #8	
6a. NAME OF PERFORMING ORGANIZATION Columbia University	5b. OFFICE SYMBOL <i>(if applicable)</i>	7b. ADDRESS (City, State and ZIP Code) Same as 8c	
6c. ADDRESS (City, State and ZIP Code) Center For Strategic Materials New York, NY 10027		9. PROCUREMENT INSTRUMENT IDENTIFICATION NUMBER AFOSR-82-0352	
8a. NAME OF FUNDING/SPONSORING ORGANIZATION AFOSR	8b. OFFICE SYMBOL <i>(if applicable)</i> NE	10. SOURCE OF FUNDING NOS.	
8c. ADDRESS (City, State and ZIP Code) Building 410 Bolling AFB Washington, DC 20332-6448		PROGRAM ELEMENT NO. 61102F	PROJECT NO. 2306
11. TITLE (Include Security Classification) Understanding The HIP Consolidation of P/M ^{Nickel} Based Superalloys		TASK NO. A1	WORK UNIT NO.
12. PERSONAL AUTHOR(S) Professor John K. Tien			
13a. TYPE OF REPORT ANNUAL	13b. TIME COVERED FROM 1 Oct 82 to 30 Sep 83	14. DATE OF REPORT (Yr., Mo., Day) 19 June 1985	15. PAGE COUNT 15
16. SUPPLEMENTARY NOTATION			
17. COSATI CODES		18. SUBJECT TERMS (Continue on reverse if necessary and identify by block number)	
FIELD	GROUP	Hot Isostatic Pressing; Alloy Powders; HIP; Consolidation	
	SUB. GR.		
19. ABSTRACT (Continue on reverse if necessary and identify by block number) Superalloy powders have been completely characterized. The different size distributions of powders have been containerized and are ready for HIP at the commercial condition of pressure and temperature, which is 15 ksi at 2050 degrees F. All creep specimens are machined and creep tests are now under way (two creep runs have already been completed). Framework for the new HIP model has been developed in order to include unequal particle sizes.			
20. DISTRIBUTION/AVAILABILITY OF ABSTRACT UNCLASSIFIED/UNLIMITED <input checked="" type="checkbox"/> SAME AS RPT. <input checked="" type="checkbox"/> DTIC USERS <input type="checkbox"/>		21. ABSTRACT SECURITY CLASSIFICATION UNCLASSIFIED	
22a. NAME OF RESPONSIBLE INDIVIDUAL DR ALAN H. ROSENSTEIN		22b. TELEPHONE NUMBER <i>(Include Area Code)</i> 202-767-4933	22c. OFFICE SYMBOL NE

DTIC FILE COPY

DTIC
ELECTE
DEC 09 1985

AFOSR-TR- 00 0984

Progress Report

for

AFOSR-82-0352

for Research in

"Understanding the HIP Consolidation of
P/M Nickel-Base Superalloys"

Research Period: 1 October 1982 to
30 September 1983

Submitted to

Dr. Ivan F. Caplan and Dr. Alan Rosenstein
Air Force Office of Scientific Research
Bolling Air Force Base
Washington, DC 20332

- June 1985 -

AFOSR-TR-85-0001

I. Introduction and Brief Progress Report

Hot Isostatic Pressing (HIP) of alloy powders to near-net-shapes is the most cost effective method of powder consolidation. Briefly, HIP involves consolidation of the powder particles at an elevated temperature and pressure; during this process, densification is known to occur principally by creep deformation of the particles [1-7]. In the superalloy case, particles of unequal size are present in the initial powder mixture, and the smaller particles undergo more extensive deformation in comparison with the larger particles [1], leaving behind undeformed boundaries of the large powder particles in the final consolidate (see Fig. 1). These undeformed boundaries, also known as prior particle boundaries (PPB), are sites for deleterious precipitation of carbide films and are partly responsible for the poor mechanical properties of the as-HIP'ed consolidate [8-10].

A step in the right direction towards resolution of this problem appears to be to maximize deformation of the particles (to break up the PPB) and to create a more uniform deformation throughout the particulate mixture. Unfortunately, at the present time, an understanding of the mechanisms of deformation during HIP and the kinetics of HIP densification is qualitative and sketchy. Also, in no study of P/M superalloys reported in the literature has the powder size or size distribution been studied as a variable in HIP consolidation. It is the purpose of this research effort to develop the necessary scientific basis that is now lacking.

During the first year of this research program (the program is now six months old), the strategy has been:



Figure 1: Prior Particle Boundaries in As-HIP'ed Rene-95.

Accession For	
NTIS CRA&I	<input checked="" type="checkbox"/>
DTIC TAB	<input type="checkbox"/>
Unannounced	<input type="checkbox"/>
Justification	
By	
Distribution /	
Availability Codes	
Dist	Avail and/or Special
A-1	



1. Characterize the powders.

2. Determine the kinetics of HIP densification at one commercial condition of pressure and temperature and for three different size distributions of particles: (a) monosized particles--for this case, the deformation can be expected to be uniform and PPB less evident; (b) bi-modal size distribution, that is, a mixture of particles of two different sizes, which is an idealization of the real case, and (c) an actual or full size distribution of particles as the standard for relative study;

3. With respect to the mechanisms of deformation during HIP, to conduct creep tests and map the regimes (in pressure and temperature) of the various deformation mechanisms (see, for example, Fig. 2). Current understanding of creep deformation of the particles during HIP is that the deformation is mainly high temperature dislocation creep. More extensive deformation can be obtained by localized superplastic flow of the powder particles during HIP, and the creep tests will determine the regimes of pressure and temperature in which superplasticity is operative.

4. Also planned for the first year was to initiate the development of a new and general analytical model for the kinetics of densification during HIP that is valid when the particles are not all of the same size.

After six months into the program, all of the above planned tasks are on schedule. The superalloy powders have been completely characterized (see Appendix A). The different size distributions of powders have been containerized and are ready for HIP at the commercial condition of pressure and temperature, which is 15 ksi at 2050°F. All creep specimens are machined and creep tests are now under way (two creep runs have already

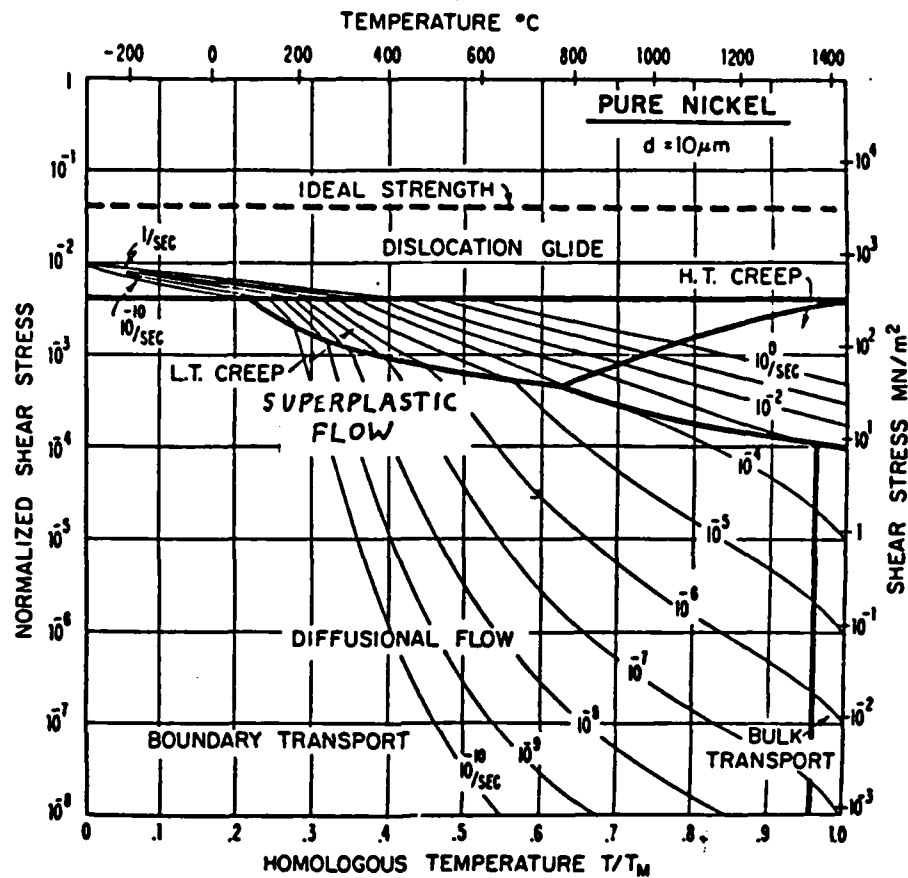


Fig. 2 . A deformation map for nickel with a grain size of $10 \mu\text{m}$. (19) A hypothetical (hypothetical because superplasticity has not been observed in nickel) field of superplastic flow has been indicated on the map by evaluating an expression for the superplastic strain rate. (20)

been completed). Finally, a framework for the new HIP model has been developed (see Appendix B) in order to include unequal particle sizes.

Already, two publications have resulted from this program. They are:

1. "Comparative Fine Structure, Microchemistry and Morphology of Rene-95 Superalloy Powders Produced by Argon Atomization and Centrifugal Atomization," J.A. Domingue, R.D. Kissinger, W.J. Boesch and J.K. Tien, to be published in the Proceedings of the Third Conference on Rapid Solidification Principles and Technologies, Gaithersburg, Maryland, December 1982.
2. "Interpretive Reivew of Comparative Microstructures and Mechanical Properties of Consolidated P/M Superalloys Produced by Modern Atomization Processes," R.D. Kissinger and J.K. Tien, same as above.

Appendix A

Characterization of Rene-95 Powder

The nominal composition of Rene-95 is given in Table AI. The powders were produced by the Argon Atomization (AA) process. The carbon level of the powders and the HIP consolidated material was 0.049 wt.%. Approximately 33% of the AA powder was -170 mesh ($<90 \mu\text{m}$) with the peak of the distribution between -400 + 500 mesh (33-38 μm). This constitutes the normal distribution. The monosized particles are approximately 85 μm in diameter (screened to a narrow size range -170 + 200 mesh, i.e., 75-90 μm powder). The bi-modal size particles were screened to -170 + 200 mesh (75 to 90 μm) and -450 to +500 mesh (33-38 μm).

Table AI

Nominal composition (wt.%) of Rene-95

C	B	Ni	Al	Ti	Cr	Co	Mo	W	Zr	Cb
.06	0.01	62.4	3.5	2.5	13.0	8.0	3.5	3.5	0.05	3.5

Relevant to the nature and rate of HIP densification is the powder particle shape and size (morphology), porosity within the particle itself, and the particle microstructure, that is, whether microcrystalline or dendritic. For example, a fine microcrystalline structure is known to promote a superplastic mode of deformation [1]. Since the prior particle boundary problem is caused by precipitation of carbide films, it is also necessary to determine the dissolved carbon content in the particles. The

results of these investigations are provided below.

a) Surface Morphology: The particles are generally spherical with many of the particles exhibiting multiple solidification initiation sites ("starbursts"). Some "satellite" structures are also evident (i.e., fine particles welded to coarse particles).

b) Porosity: The percent of particles with central pores (see Fig. A1) for various particle diameters is given in Table AII. Thus, except for small particle sizes ($<10 \mu\text{m}$), the % volume occupied as enclosed porosity appears to be significant. Table AIII shows how interdendritic shrinkage voids are distributed as the particle diameter varies. It needs to be determined how the enclosed porosity affects the densification kinetics and the mechanisms of deformation responsible for the densification.

Table AII
Percent Particles with Central Pores

Particle Diameter μm	%
215	65
170	67
125	44
100	45
65	14
35	5

Table AIII
Distribution of Interdendritic Shrinkage Voids

Particle Diameter μm	Distribution
200-230	Throughout particles
97-104	Only near surface
33-38	none observed

c) Sectioned Particle Microstructures: As indicated in Table AIV, the particles are essentially dendritic (see Fig. A1) for the larger particle sizes with the microcrystalline and cellular structures more probable at smaller particle size ranges.

d) Dissolved Carbon and Carbide Content: MC type Nb-rich carbide was extracted by digesting the powder specimens with 10 vol.% bromine methanol. Carbon analyses were performed on the residues to determine wt.% of alloy carbon fixed as MC, and the remainder of the carbon was assumed to be dissolved. In this work dissolved carbon was found to stay at about 20% for close sieve fractions down to 150 μm , below which it increased. X-ray diffraction showed no crystalline phases other than MC in the residues. Thus, the tendency for carbide precipitation during HIP can be expected to increase as particle size decreases. On the other hand, the extent of deformation also increases for the smaller particles, so that PPB effects can be seen to be a trade-off between the two opposing tendencies.

Table AIV
Cooling Microstructures

Particle Diameter	Dendritic	Cellular	Microcrystalline
μm	%	%	%
107	100	-	-
38	95	5	-
12	90	9	1

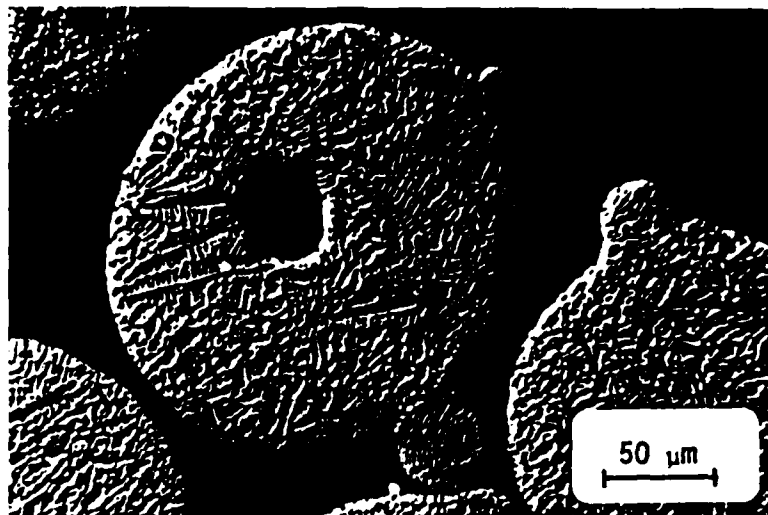


Figure A1: Argon atomized Rene-95 powder shows a central enclosed pore within the powder particle. A dendritic structure and "satellite" particles are evident also.

Appendix B

Analytical Developments

A rough initial working model for the densification mechanism map is that of Artz et al. [7]. This model does not take into account superplastic flow regimes and is valid only for the monosized particle case. For the case of the bi-modal or the more general particle size distribution case, two very basic equations of the Artz et al. model become invalid. One is the equation for the particle coordination number Z and the second, the equation relating the interparticle force (f) to the applied pressure (p). In general, Z can be given by the cumulative radial distribution function for a random dense packing, G , and Artz et al. utilized the experimentally obtained linear approximation for G for the monosized particle case given by

$$G(r) = Z_0 + C(r/2R - 1) \quad (B1)$$

where Z_0 , C are constants and R is the particle radius. In principle, this experimental result is not any more reliable than accurate theoretical predictions, and, strictly, $G(r)$ must be evaluated from

$$G(r) = \int_0^R g(r) 4\pi r^2 dr \quad (B2)$$

where $g(r)$ is the radial distribution function and has been exactly evaluated for a random dense packing of spheres both for the monosized particle case [12-14], the bi-modal particle size case [15,16], and also for the more general case of a mixture of n particle sizes [15,16].

With respect to the interparticle force, the equation used by Artz et al. [7] is that derived by Molerus [17] for the monosized particle case and given by

$$f = 4\pi R^2 p / ZD \quad (B3)$$

Following Molerus [17], an equation was derived for the bi-modal particle case and is given here without derivation by

$$p = (FD/4\pi) [Z_1 / (r_1^2 + f_2 R_2^2 / f_1) + Z_2 / (r_2^2 + f_1 R_1^2 / f_2)] \quad (B4)$$

where Z_1, Z_2 are the coordination numbers of particles 1 and 2, f_1, f_2 the respective number fractions and R_1, R_2 the respective particle radii. If the particle sizes are not too different $Z_1 = Z_2 = Z$; however, when the sizes vary considerably, the smaller particles can be expected to sit in the interstices of a random packing of the larger particles [18] and, in this case, the rigorous expressions for $g_1(r)$ and $g_2(r)$ must be used for Z_1 and Z_2 . Densification mechanism maps using this approach will be developed.

END

FILMED

1-86

DTIC